CHAPTER-2
RESOURCES AND METHODS

2.1 Databases

2.1.1 European ST-T Database (EDB)

The European ST-T Database (EDB) records are expected to be employed to assess the performance of the developed technique of validation outcomes. This collection comprises 90 ECG recordings from 79 patients, each annotated beat by beat. The respondents are 8 women between the ages of 55 and 71 and 70 men between 30 and 84. For each subject, additional selection criteria were created, including baseline ST segment displacement, to diagnose myocardial infarction. The database contains 367 episodes that correspond to an ST segment change. These episodes can last from 30 seconds towards many minutes in length.

Additionally, maximum deflections from 100 μV to more than one mV have been described. The compact clinical reports document, which covers medicine, technical information, pathology, and electrolyte imbalance, is included as a header (.head) file in each record. The header documents incorporate data about the patient's age, gender, recording leads, medications, gear, other details, diagnostic tests, and the recording equipment. This dataset is a two-hour collection of channels at a sampled speed of 250 samples per second, with a 12-bit resolution and a minimum 20 mV data spectrum. Following digitization, the sample values were rescaled to provide all ECG signals with a constant size of 200 ADC units for every mV. The size of each ECG signal record is 5,400,000 bytes. Each recording was examined beat by beat for changes in ST fragmentation by two impartial cardiologists. Annotated ST segments identified both leads' onsets, extremes, and endings. After comparing the annotations of two experts, the Pisa program was used to resolve any differences, and the final reference annotation records were created. In total, there are 802,866 annotations in these 90 records [A. Taddei, 1992]. According to the database, two leads were obtained from the V1, V2, V3, V4, V5 and MLI, MLI places. The European Society of Cardiology Three defines Ischemic Episodes. Experienced medical doctors were brought together to create a set of guidelines for determining the period of ST episodes with considerable ST segment displacement in the ECG signal. The following criteria [A. Taddei, 1992] was employed to detect and annotate an ST

episode:

Each participant's ST segment deviations are analyzed about a reference signal (usually selected from the first 30 seconds of each record). The ST segment deviation is measured 80 milliseconds after the J point, whereas if the heart rate is less than 120 beats per minute. And 60 milliseconds just after J point if the heart rate is larger than 120 beats per minute.

- When the apparent ST deviation is much less than 0.1 mV, there must be a minimum time of 30 seconds between ST episodes.
- Every episode of ST has a heading at the beginning. The beginning can be determined by shifting away from the moment when the overall ST deviation first reaches 0.1 mV. The research goes on until a pulse is discovered that has an overall ST deviation of less than 0.1 mV and a complete ST deviation of less than 0.05 mV during the previous 30 seconds. An ST-T deviation shows the start of the episode comes right after this beat.
- The highest positive or negative divergence for each ST episode is recorded. A typical evaluation of the biggest ST deviation is included in an ST change annotation appended from the rhythm preceding the one with the greatest ST divergence.
- At the final moment of each ST episode, an annotation is provided. Looking forward from when the complete ST deflection was only last greater than 0.1 mV leads to the conclusion. The search continues until a rhythm with an absolute ST deviation of lower than 0.05 mV is discovered, followed by a beat with a complete ST deviation of lower than 0.1 mV for the next thirty seconds. This beat immediately precedes an ST transition annotation indicating the episode's conclusion.
- Each ST change annotation has a text section that focuses on the significance of the change. The text message contains the symbols for the event type ('ST,' the signal number ('0,' or '1), and the deviation's position ('+' or '-'; high T variations are denoted by '++' and '—'). The text field of an annotation that denotes the beginning of an episode has a ' prefix'. There is a prefixed "A" and an additional three or four-digit number that indicates the size of the greatest deviation in microvolts for an annotation that denotes the conclusion of an episode. MIT-BIH Database.

2.1.2 MIT/BIH database (Massachusetts Institute of Technology/Beth Israel Hospital)

This dataset includes hundreds of electrocardiogram (ECG) recordings totaling more than 200 hours in length. Individual recordings range from 1 to 3 signals; in length, it is from 20 seconds to more than 24 hours. Most of these recordings are roughly 30 minutes long, feature two signals, and are beat-by-beat annotated. A header, signal, and annotated file characterize most ECG recordings. A record is made up of these three files. These documents are organized into nine databases, each with its directory. Each database entry contains a continuous recording from a single subject.

Record names

100 101 102 103 104 105 106 107 108 109 111 112 113 114 115 116 117 118 119 121 122 123 124

200 201 202 203 205 207 208 209 210 212 213 214 215 217 219 220 221 222 223 228 230 231 232

During 1975-1979, the Arrhythmia Laboratory at BIH in Boston investigated 48 annotated recordings from 47 subjects in this collection. Almost 60% of these documents were acquired from inpatients. The dataset (the "100" series) has 23 records that were chosen at random from a set of around 4000 24-hour Holster records. To include a variety of therapeutically relevant occurrences that are also uncommon and would not be well described by a small representative sample, 25 records (the "200" series") from the set were chosen. Because aspects of the rhythm, QRS shape, or signal quality can make arrhythmia detection challenging, the recordings in the 200 sequence have been found primarily. The average length of a single record is roughly 30 minutes. Every signal file usually has two 360 Hz samples. The data type contains information about the used connections, as well as the age of the patient, gender, and medications.

2.2 Methods

2.2.1 Savitzky-Golay

This research introduces the powerful statistical technique Savitzky-Golay, which may be applied to various engineering problems, and shows how it is employed in a

technical experiment. It is based on comparing two methods: the Savitzky-Golay average polynomial smoother and the polynomial regression model. The moving averages approach is one of the most basic and often utilized extrapolation techniques. A moving average is a technique of straightening datasets by aggregating a set record for consecutive contexts (with or without weights). Moving averages are employed to sort out series data variants or identify series data elements such as pattern, loop, and seasonality. A moving average is a method for identifying patterns in a data set. The moving average is especially suitable for determining long-term trends [S.C.H. Albricht and W.L. Winston, 2015]. The easiest method of smoothing time series is probably primary (unweighted) moving average smoothing. However, it has many significant flaws. One of them is that a moving average always trails the most recent observation, which means that old observations dropping out of the average might have a disproportionate impact on the moving average. The end-point problem is relevant. The simple moving average method is the most useful when it comes to moving averages.

There is no apparent seasonality or trend in demand. Aside from these two drawbacks, weighted moving average smoothing has additional drawbacks. Notably, selecting the weighted moving average greatly affects the results. When employing this method, the best feasible weighting factors should be discovered iteratively; however, the weighting factors are frequently chosen to give greater weight to more recent data. However, the collection of weighting elements is generally irregular [W. Brock and J. Lakonishok, 1992] [T. Kwaak and W. Liebregts, 2012]. The span has an important role. When the time range is long, such as 12 months, many observations are incorporated into each average, and extreme values have little impact on forecasts. The resulting forecast series will be significantly smoother than the previous one. When the time range is short, such as three months, severe observations have a greater impact on the forecast, and the forecast series is less smooth.

Moving averages based on these criteria should become significantly less effective as observations get older, whereas weighted moving average smoothing distributes mathematically increasing weights over time. The latest assumptions are weighted more heavily than faraway findings. One or more smoothing parameters are computed on how often weightage is given to each analysis to achieve imbalanced weighting.

The simplest of these techniques is simple exponential smoothing, ideal for a sequence that moves randomly above and below a consistent mean (stationary series). No clear seasonal trend or pattern can be found [E. Ostertagova, 2015].

Then there is double exponential smoothing, which is commonly used, although it is best to avoid it when there's a seasonal tendency. Because it considers both seasonality and trends, triple exponential smoothing (also known as Holt-Winters smoothing) is the most comprehensive type of exponential smoothing. The choice of the smoothing factors is arbitrary for exponential smoothing as well. However, choosing the value that minimizes the mean of squared errors MSE [W. Brock, J. Lakonishok, and B. Lebaron, 1992] is fair. Moving average filters are widely used in the industry to analyze noisy data in real-time. Savitzky-Golay's moving average smoothing filter is obtained from the least squares fit of a lower-order polynomial to a set of successive points. The inventors claim that discrete convolution with a constant IIR filter is analogous to matching a polynomial to a collection of input samples and evaluating the resulting polynomial at a single point inside the approximation interval. Savitzky and Golay have been involved in levelling nonlinearities from synthetic frequency band analysis tools, and they showed that straightening least-squares decreases artifact whereas preserving waveform peak shape and height (in their case, Gaussian-shaped spectral highs) [S. Balan, A. Khaparde and V. Tank et.al, 2014]. A least-squares fit to a higher-order polynomial is performed with exponential smoothing, while a least-squares accommodate to a higher-order polynomial is performed with SG filters. The higher the polynomial order, the larger the smoothing window. A second-order (quadratic) SG filter is preferable if the data in a given smoothing window fits a parabola. A fourth-order (quartic) SG filter is commonly used when the data provides a fourth-order polynomial. The preservation of crucial original time series properties, such as comparable widths and heights, is a significant benefit of this method. Other (simpler) averaging strategies usually flatten these traits. If the data is unevenly spaced, a least-squares fit must be performed within a window size over each data set. The theory of Savitzky-Golay polynomial smoothing and its application to a specific situation was presented. The Savitzky and Golay data straightening approach is based on least-squares polynomial approximation. Under the right circumstances, the SGMA polynomial smoother will achieve a decent waveform smoothing trade-off. These are the polynomial degree and window sizes that are

adequate.

The coefficients for each polynomial order must be calculated so that the appropriate polynomial curve best matches the available data. Using the least square method appropriate for such a limited set of successive pieces of data to a polynomial rather than an averaging filter is preferable. As a result, the least-squares fit technique is used to select polynomial coefficients that result in the smallest sum of squared errors. To replace the original data, the output smoothed value is obtained at the center of the window [S. Balan, A. Khaparde et.al, 2014]. Frequency data or spectroscopic (peak) data are frequently used in the Savitzky-Golay filtering procedure. This method works well for frequency data because it restores the high-frequency components of the signal. To de-noise, the Savitzky-Golay approach can be less effective than a moving average filter. However, it is essential to note that a higher degree polynomial can provide significant normalization without reducing data features.

2.2.2 Wavelet Transform

The Wavelet transform [A. Graps, 1995] represents the wavelet function. The daughter wavelet will first scale and convert this wavelet function into a chunk of information using a fixed-length signal designated as the mother wavelet transform. However, using the wavelet transform, a given continuous signal is split into several size components with a unique frequency range. Every frequency-scaled component is then destined with a resolution known as a multi-resolution analysis (MRA).

In the time domain, the mother wavelet function is defined to be significant within a specific frequency range and zero elsewhere [C. Lin et al., 2010]. The properties of the mother wavelet have zero- mean and normalization, as shown in Eqns. (2.1) and (2.2).

$$\int_{-\infty}^{\infty} \Psi(t)dt = 0 \qquad (2.1)$$

$$\int_{-\infty}^{\infty} \Psi(t)\,\Psi^{*}(t)dt = \|\Psi(t)\|^{2} \qquad (2.2)$$

According to the delineation and interpretation properties Eqn. (2.3), the wavelet function canrepresent a basis function indicated by Eqn. (2.3).

$$\Psi_{s,\mu}(t) = \frac{1}{\sqrt{s}}\Psi\left(\frac{t-u}{s}\right)\Big|\ \mu, s \in R \qquad (2.3)$$

When the S-scaling parameter (T) is the translation having a value higher than zero since negative scaling is disregarded. The multi-resolution wavelet transform has orthonormal properties achieved by set (T) the co-efficient of the persistent wavelet transform to the co-efficient of the basis (T) as follows: Wf(u,s)=<f(t), $\Psi_{s,\mu}$ >

$$\int_{-\infty}^{\infty} \mathrm{f(t)}\ \Psi^{*}\ (t)dt \qquad (2.4)$$

$$\int_{-\infty}^{\infty} \mathrm{f(t)}\ \frac{1}{\sqrt{s}}\Psi^{*}\left(\frac{t-u}{s}\right)dt \qquad (2.5)$$

The two-dimensional co-efficient W(f(s,u)) mentioned in Eqn. (2.4) can be mapped from the single-dimensional signal f(t) using the wavelet transform. These factors are used to undertake both frequency and time analysis simultaneously. As a result, we can occupy a specific frequency (with s) at a particular time (with u). The Fourier transform of Ψ (t) is Ψ (w) called the mother wavelet mentioned in Eqn. (2.5). This equation is also acknowledged as an admissibility condition. The Wavelet transforms are categorized into two categories: discrete Wavelet transforms, and continuous Wavelet transforms. It should be noticeable that DWT and CWT are both continuous transforms. The continuous-time signal can be represented by using this transform.

The discrete wavelet transform employs an especially scale grid and translation, whereas the continuous wavelet transform tends to work throughout every translation grid and scale possible. A signal obtained from various resources employing various transducer electrode materials cannot be predicted effectively using an effective outcome. The primary goal of processing is to extract valuable data for signal prediction. It is typically accomplished or gained by transforming the original into different domains to interpret the ECG signal's characteristics accurately. The original signal can be obtained by using the inverse transformation of the inverse transform of the divided signal without losing the most sensitive information. Other methods and widespread transformation in biomedical signal processing include short-time Fourier transforms (STFT), Fourier transforms (FT), and wavelet transforms. By using these, transform all the signals mapped into one way. The advantages of these transforms can be used to analyze a specific signal [R. Polikar, 2000]. The wavelet transform has benefits over the STFT and FT regarding proper deconstruction and restructuring; it

also has the upper hand in being non-fixed and non-periodic.

2.2.2.1 Approximations and Detail Co-efficient

The low and high-frequency co-efficient is present for proper ECG signal assessment. Usually, we talked about the approximation and detail co-efficient in wavelet analysis. The high-frequency component of the low scale of signal analysis is the detail co-efficient. The short-wavelength components and slightly elevated scale of analyzing signals are the approximation co-efficient. The process of filtering [I. Daubechies, 1990; S.G. Mallat and S. Zhohgs, 1989; T.N.G. Strang, 1996] at its most fundamental level, as shown in Figure 2.1.

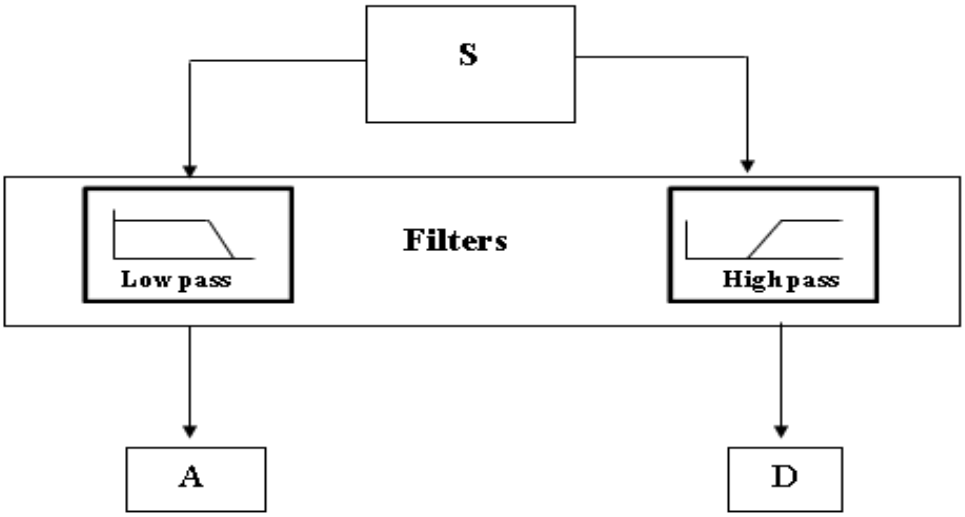

Figure 2.1 Approximations and details co-efficient after signal filtration
[reproduced from http://in.mathworks.com/discrete-wavelet-transform.html]

Let us consider the input signal ‘s’ having 1000 samples, and this signal ‘s’ passed through the two filters. After applying the wavelet, the resulting signals out of a total of 2000 signals having each signal 1000 samples. These signals are broken down into approximation and detail co-efficient using the wavelet transform. By this co-efficient, we can maintain a single signal in control to get all the data from the separated signal. This is referred to as down-sampling. This process generates the two sequences ‘CD’ and ‘CA’. The down-sampling generates the two DWT coefficients, as shown in Figure 2.2. By using this process, we gain better results, so there is discrete wavelet transform decomposition has been performed for one phase.

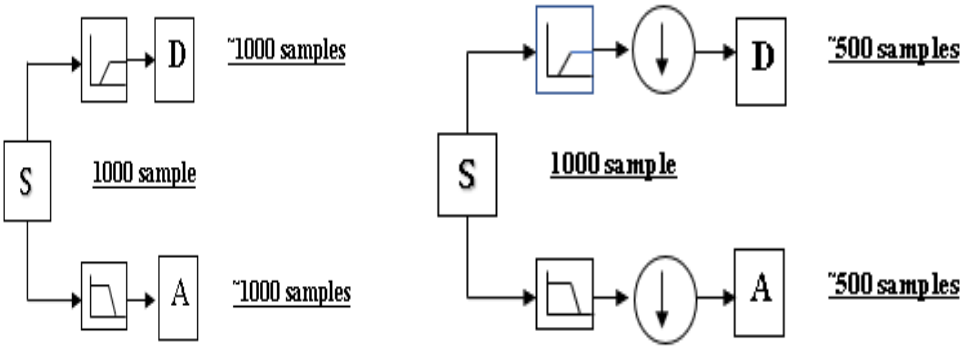

Figure 2.2 Diagram of down-sampling [reproduced from http://in.mathworks.com/discrete-wavelet-transform.html]

Figure 2.3 depicts a wavelet decomposition process for a sinusoidal signal with a very high - frequency**.**

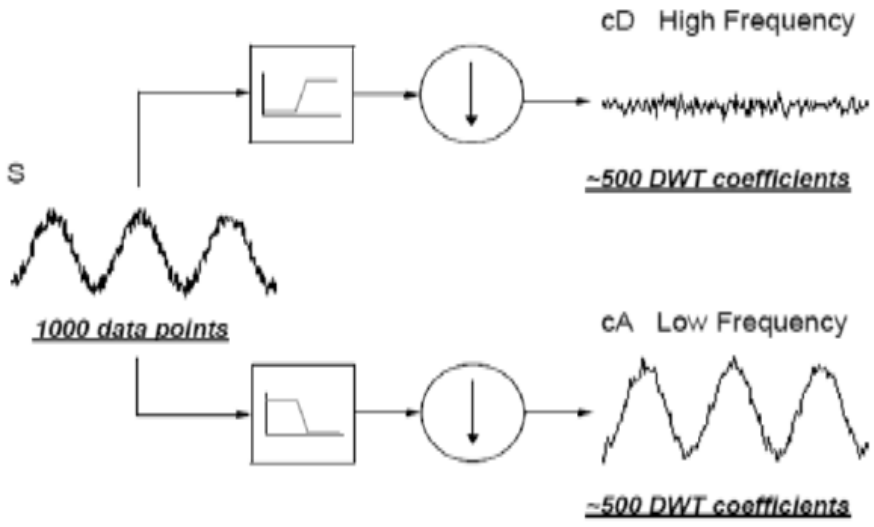

Figure 2.3 Real-time wavelet decomposition [reproduced from http://in.mathworks.com/discrete-wavelet-transform.html]

2.2.2.2 Multiple level Decomposition

The decay strategy is usually repeated until serial communication components are decomposed up to the requirement of lower-resolution components. The decomposition up to multiple levels is known as a wavelet decomposition tree, as shown in Figure 2.4.

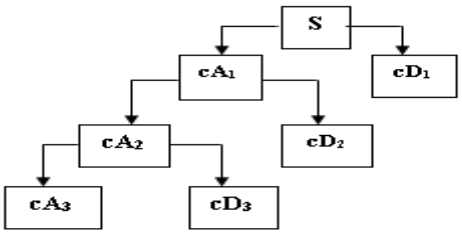

Figure 2.4 Decomposition of multiple levels [reproduced from http://in.mathworks.com/discrete-wavelet-transform.html]

2.2.2.2.1 Number of Levels

The examination cycle was rehashed endlessly. This procedure is known as iteration. The decay strategy can sometimes be directed till every detail co-efficient is composed of a single sample of analyzing messages. In other cases, the decomposition with the equivalent number of levels is required depending on the info from the biomedical signals, as shown in Figure 2.4.

2.2.2.3 Reconstruction of Wavelet Transform Signal

By employing DWT, the original signal is decomposed; this process is called analysis and decomposition. The decomposed and analyzed wavelet coefficients have reconstructed the original signal without losing essential or privileged data. As illustrated in Figure 2.5, this procedure is called synthesis and reconstruction.

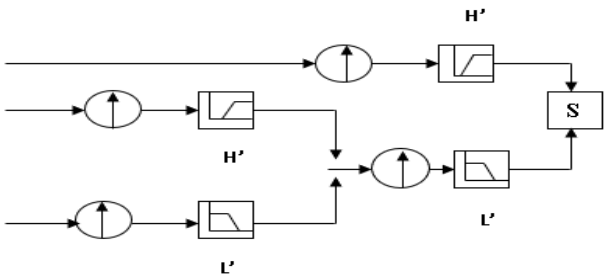

Figure 2.5 Wavelet reconstruction [reproduced from http://in.mathworks.com/discrete-wavelet-transform.html]

The IDWT (inverse discrete wavelet transforms) is manipulated mathematically, influencing the synthesis process. The original signal can be synthesized using wavelet toolbox software from detailed and approximate co-efficient. Generally, the wavelet transform used to analyze the original signal includes down-sampling and

filtering, while the wavelet reconstruction process involves up-sampling and filtering. Further, the up-sampling process is called lengthening a unique signal by interpolating zeros between both samples. As shown in Figure 2.6 example of up-sampling is presented.

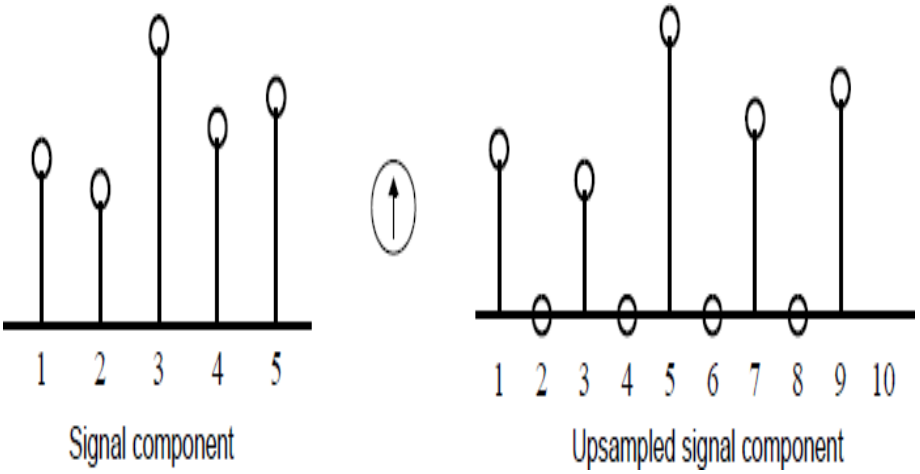

Figure 2.6 Up-sampling of the signal [reproduced from http://in.mathworks.com/discrete-wavelet-transform.html]

2.2.2.4 Reconstruction Filter

Down-sampling (decomposition) adds up the noise in the original signal, called aliasing. During the decomposition and reconstruction phases, a proper filter should be chosen to remove or degrade the aliasing effect. Figure 2.7 illustrates the location of the quadrature mirror filters in the low and high pass decomposition filters (L and H), as well as the reconstructed filters (L' and H').

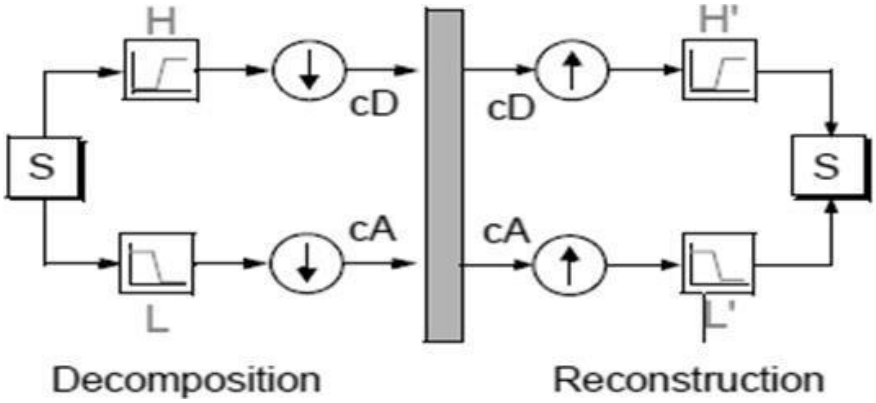

Figure 2.7 Quadrature mirror filters [Reproduced from http://in.mathworks.com/wavelet-reconstruction.html]

2.2.2.5 Approximation and Details Reconstruction

The possibility of reconstruction of the input signal using low pass filter co-efficient (detail) andhigh pass filter (approximations) co-efficient as shown in Figure 2.8.

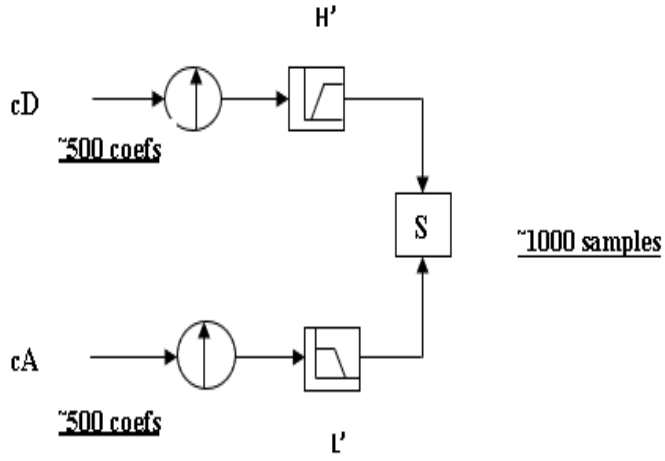

Figure 2.8 Reconstructing approximations and details co-efficient [Reproduced from http://in.mathworks.com/wavelet-reconstruction.html]

Additionally, it is possible to recreate the approximation and detail coefficients using their respective vector coefficients. The justification for this method is shown in Figure 2.9. The reconstruction of the exact first-level approximations (A1) from cA1 is shown in this picture (approximation co-efficient vector). Instead of cD1, provide the zeros vector (details co-efficient).

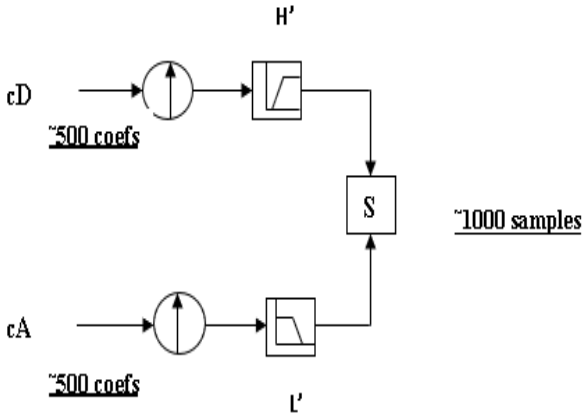

Figure 2.9 Reconstructing approximations and details with approximations [Reproduced from http://in.mathworks.com/wavelet-reconstruction.html]

For obtaining the input data S combine both the original signal by cD1 and cA1 as given in Eqn. (2.6) and shown in Figure 2.10.

$$A1+D1=S \quad (2.6)$$

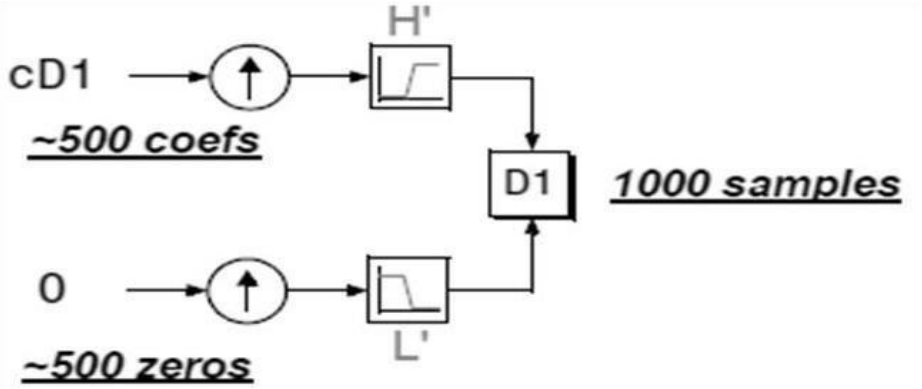

Figure 2.10 Reconstructing approximations and details with approximations being zero's [Reproduced from http://in.mathworks.com/wavelet-reconstruction.html]

Noticing that the co-efficient coordinate values 'cA1' and 'cD1' are generated using down-sampling. The reconstruction of approximation and detail must be co-efficient before adding them. Similarly, for the multilevel evaluation method, determine the equivalent interaction procedure for all retrieved signal co-efficient. Figure 2.11 depicts an example of this procedure.

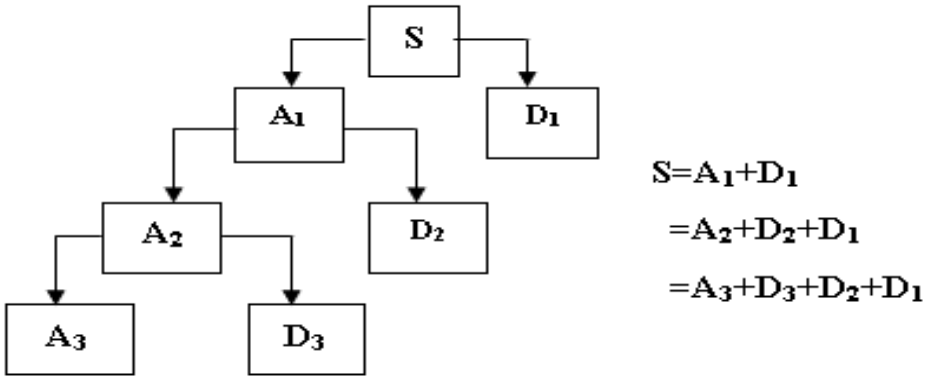

Figure 2.11 Reconstructed signal components [Reproduced from http://in.mathworks.com/wavelet-reconstruction.html]

2.2.2.6 Multi-Level of Decomposition and Reconstruction

The reconstruction and decomposition of the multi-step (evaluation and formulation) procedure have been shown in Figure 2.12. This procedure has two stages; the first

one: Breaking up of original signal and calculating the wavelet co-efficient obtained from the achieved co-efficient.

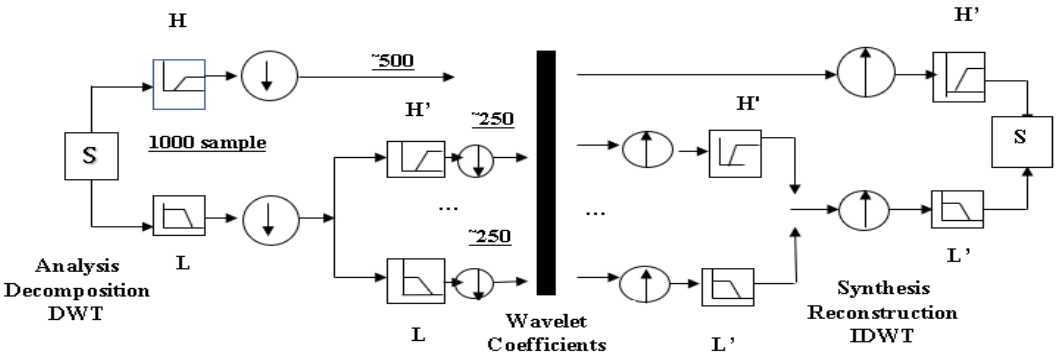

Figure 2.12 Multistep analysis-synthesis process [Reproduced from http://in.mathworks.com/wavelet-reconstruction.html]

To achieve co-efficient having many applications, wavelets transform analysis is used, and de-noising is the first among them.

2.2.2.7 Frequency and Scale

Different scales in wavelet transform have various frequency ranges. More of the input signal is taken into account as the wavelet is extended, and, in this way, the tough signal features are considered by the wavelet co-efficient [I. Daubechies, 1990]. As a result, the wavelet analysis reveals a relationship between the frequency and wavelet scales.

2.2.2.8 DWT (Discrete Wavelet transform)

It is challenging to figure out the wavelet coefficient at each dimension. It creates useless data. It comes to light that choosing one position and scales-based power of two is known as dyadic positions and scales. As a result, the solution will become more precise and efficient. This solution is made possible by the DWT (Discrete Wavelet transform). It is a good technique for the implementation of this method using filters. The development of this technique was processed by Mallet in 1988 [S.G. mallet, 1989]. In signal processing society, the mallet algorithm is a standard scheme that acts as sub-band codes for two channels [C. Lin et al., 2010]. This filtering-based method generates a fast wavelet transform.

The wavelet function and scaling are explained by the basis functions of Daubechies, Haar, and others. It is possible to approximate the discrete signal by Eqn. (2.7).

$$f[n] = \frac{1}{\sqrt{M}} \sum_k W_{\emptyset}\left[j_0,k\right] \emptyset_{j_{0,k}}[n] + \frac{1}{\sqrt{M}} \sum_{j=j_0}^{\infty} \sum_k W_{\Psi}\left[j,k\right] \Psi_{j,k}[n] \qquad (2.7)$$

For obtaining the wavelet co-efficient, we can take simply the inner product as given in Eqns. (2.8) and (2.9)

$$W_{\emptyset}\left[j_0,k\right] = \frac{1}{M} \sum_n f[n]\, \emptyset_{j_{0,k}}[n] \qquad (2.8)$$

$$W_{\Psi}\left[j,k\right] = \frac{1}{\sqrt{M}} \sum_n f[n]\, \Psi_{j,k}[n] \quad j \geq j_0 \qquad (2.9)$$

2.2.2.9 Fast Wavelet Transform

In general, the scaling and wavelet functions are well understood and its wavelet co-efficient canbe easily achieved in Eqns. (2.8) and (2.9). One can find a different way to find the wavelet coefficients without knowing the scaling and the dilation function [C. Lin et.al, 2010]. The calculation time can be reduced..

$$\emptyset_{j,k}[n] = 2^{\frac{j}{2}}\, \emptyset\left[2^j n - k\right]$$

$$= \sum_n h_{\emptyset}[n]\, \sqrt{2}\emptyset\left[2\left(2^j n - k\right) - n\right] \qquad (2.10)$$

Let $n' = m - 2$, we have

$$\emptyset_{j,k}[n] = \sum_m h_{\emptyset}[m - 2k]\, \sqrt{2}\emptyset\left[2^{j+1} n - m\right] \qquad (2.11)$$

If we combine Eqns. 2.10, 2.11 and Eqn. 2.8

$$W_{\emptyset}\left[j,k\right] = \frac{1}{\sqrt{M}} \sum_n f[n] \emptyset_{j,k}[n]$$

$$= \frac{1}{\sqrt{M}} \sum_n f[n]\, 2^{\frac{j}{2}}\, \emptyset\left[2^j n - k\right]$$

$$= \frac{1}{\sqrt{M}} \sum_n f[n]\, 2^{\frac{j}{2}} \sum_m h_{\emptyset}[m - 2k]\, \sqrt{2}\emptyset\left[2^{j+1} n - m\right]$$

$$= \sum_m h_{\emptyset}[m - 2k] \left(\frac{1}{\sqrt{M}} \sum_n f[n]\, 2^{\frac{j+1}{2}}\, \emptyset\left[2^{j+1} n - m\right]\right.$$

$$= \sum_m h_{\emptyset}[m - 2k]\, W_{\emptyset}[j + 1, m] \qquad (2.12)$$

$$= h_{\emptyset}[-n] * W_{\emptyset}[j + 1, n] | n = 2k, k \geq 0 \qquad (2.13)$$

Similarly, for detail co-efficient Eqn. (2.14) it is.

$$W_{\Psi}[j,k] = h_{\psi}[-n] * W_{\emptyset}[j+1,n]n = 2k, k \geq 0|n = 2k, k \geq 0 \quad (2.14)$$

For discrete signal, the data and original signal can be considered approximate co-efficient with order] i.e. f[n]=W [j, n] is representation by Eqn. (2.12) and Eqn. (2.13). The next level of approximation and detail can be obtained. This algorithm is 'fast' because one can find the coefficient level by level rather than directly using Eqn. 2.8 and 2.9 [C.L. Liu, 2010].

2.2.2.10 Comparison between Wavelet Transform-based analysis and the Fourier Transform, Short Time Fourier Transform

2.2.2.10.1 Fourier Transform based Analysis

Signal analysts already have in their discarding an impressive armory of tools. Possibly, the most well-known technique of these is Fourier analysis as shown in Figure 2.13. This method breaks down an original signal into ingredient sinusoids of different frequencies. The Fourier analysis is a mathematical method using Eqn. 2.15 for transforming the original signal to frequency based from time based [R. Polikar, 2000]

$$H(\omega) = \int_{-\infty}^{\infty} f(t)e^{-i\omega t}dt \quad (2.15)$$

Where H(ω) is the Fourier transform of a signal f(t).

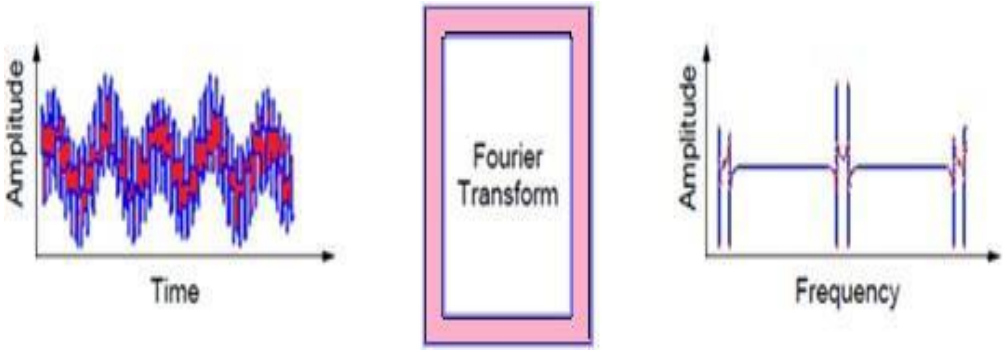

Figure 2.13: Fourier transform [reproduced from http://in.mathworks.com/discrete-wavelet-transform.html]

For numerous signals, Fourier analysis is tremendously helpful because the signal's frequency content is of immense significance. Fourier analysis has a serious hitch, time information is lost when transforming to the frequency domain. Another hitch includes, it is impracticable to notify a particular event took place. This hitch is not very important for a stationary signal. However, the most physiological interesting signals

hold frequent non-stationary or transitory characteristics include abrupt changes, drift, trends, beginnings and ends of events. These individualities are usually the most important part of the physiological signals; hence Fourier analysis is not appropriate for detecting them.

2.2.2.10.2 Short Time Fourier Transform based Analysis

In an effort to correct above mentioned deficiency, Dennis Gabor tailored the Fourier transform, to analyze only a small section of the signal at a time, called windowing the signal as shown in Figure 2.14. This adaptation is known as Short Time Fourier Transform (STFT) as mentioned in Eqn. 2.16. It maps an original signal into a 2-dimensional signal, which is a function of frequency as well as time. STFT employs a frequency-time depiction 'H(ωτ)'of the continuous time signal 'f(t)', Eqn. 2.16.

$$H(\omega,\tau) \int f(t)g(t-\tau)\, e^{-i\omega t}dt \qquad (2.16)$$

Where g(t-τ) is a window function

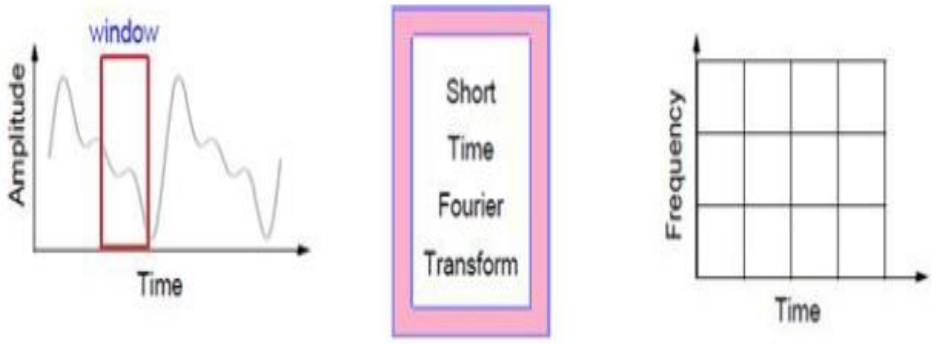

Figure 2.14: Short time Fourier transform [reproduced from http://in.mathworks.com/discrete-wavelet-transform.html]

The STFT represents a sort of concession between the frequency and time-based view of a signal. It provides information in short, at what frequencies and when a signal event occurs. Though, one can only get this information with limited precision, as precision is decided by the size of the window. On the other hand, the STFT concession between frequency and time information can be useful. The disadvantage of STFT include, once a meticulous size of the time window has been chosen, the time window will remain same for all frequencies. A lot of signals need a more flexible approach, where the variation of the size of the window is primarily required to find more accurate either frequency or time or both based information at a time.

2.2.2.10.3 Wavelet Transform based Analysis

Wavelet analysis represents the next logical step to STFT analysis. This analysis involves a windowing technique with variable sized regions. It allows the use of long-time intervals where one wishes shorter regions, whereas one wishes high-frequency information or more precise low-frequency information as shown in Figure 2.15.

Figure 2.15 Wavelet transform [reproduced form http://dsp.stackexchange.com/wavelet-transform]

Here's what this looks similar to in contrast with the frequency-based, time-based and STFT views of an original signal:

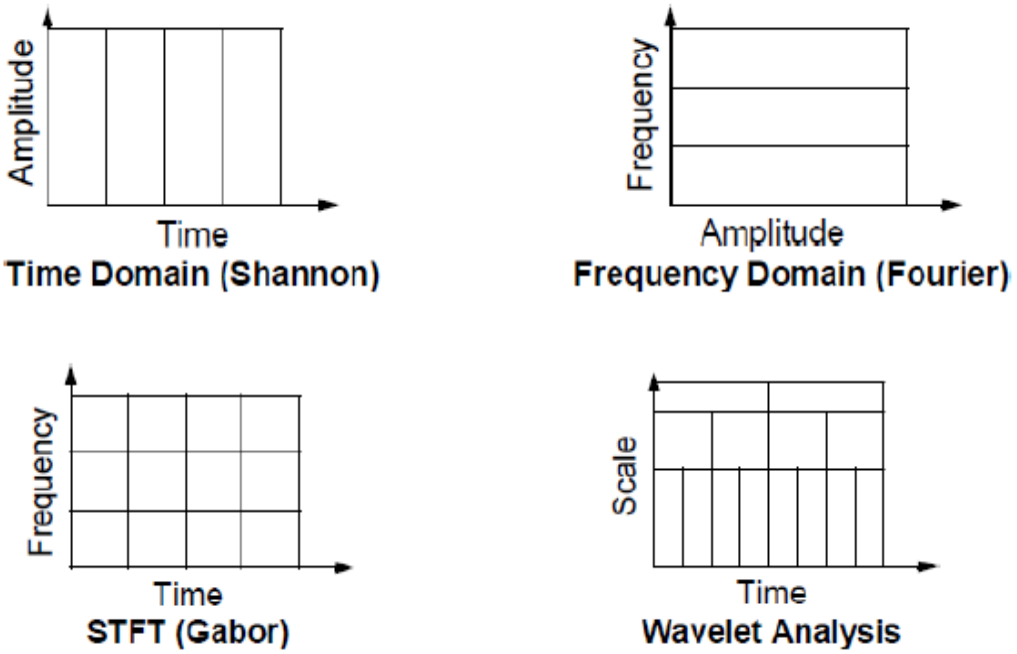

Figure 2.16 Time, frequency domain, STFT vs. wavelet transforms based analysis [reproduced form http://dsp.stackexchange.com/wavelet-transform]

Here, a noticeable point about the wavelet analysis is that, it does not use a frequency-time region, but somewhat a scale-time region. This analysis is capable of

enlightening aspects of other than signal analysis methods. This analysis is used detection of breakdown points, discontinuities in higher derivatives, trends and self-similarity. In addition, wavelet analysis can de-noise a signal without significant degradation as compared in Figure 2.16.

2.2.2.11 Characteristics of wavelet transforms

The varying features of wavelet transform are portrayed underneath (W. Sweldew and J. Kovacevic, 2010)

- Regularity
- The window's function is the fewest outside scheduled time that contains the activity nil.
- The orthogonal filter serves as the orthogonal wavelet basis function's guide, and the wavelet transform's result is energy-preserving.
- The haar wavelet is the only wavelet transform with symmetric properties in transverse.
- In the case of bi-orthogonal wavelets, however, both the wavelet function and the scaling are anti-symmetric or symmetric.
- Several vanishing events calculate the order of approximation of the polynomial.
- The wavelet support in time, rate of decay, frequency, and the reconstruction filter has their linear phase.
- A broad group of signals includes the number of increasing events, the wavelet with several growing events, and the wavelet's sparse signal representation.
- Iterative algorithms are used for wavelet development to congregate quicker and ensure a scaling function's presence.

2.2.2.12 Families of Wavelet Transform

Wavelet families have been categorized into five types, i.e., the fundamental types of mother wavelets.

- Crude wavelets: Mexican hat, Morlet, Gaussian
- Orthogonal & Compactly supported wavelets: Coiflets, Symlet, Daubechies
- Infinitely irregular wavelets: Dmeyer, Meyer
- Complex wavelets: Complex Shannon, Complex frequency B-spline, Complex Gaussian,Complex Morlet
- Bi-orthogonal & Compactly supported wavelet pairs: Bi-orthogonal, Reverse bi-orthogonal

The following are the relevant characteristics of such wavelets (I. Daubechies, 1990; R. Janani, 2014):

Haar

Symmetry, scaling function, compactly supported orthogonal, bi-orthogonal investigation, orthogonal examination, continuous and discrete time change, exact reconstruction, explicit expression, FIR filters, fast algorithm.

Daubechies

Compactly supported orthogonal Arbitrary regularity, asymmetry, orthogonal analysis, an arbitrary number of vanishing moments, bi-orthogonal examination, FIR filters, accurate reproduction, fast algorithm, continuous and discrete time transformation, scaling function

Coiflets

A number of vanishing moments, compactly supported orthogonal, vanishing moments for scaling function, arbitrary regularity, orthogonal investigation, scaling function, bi-orthogonal examination, fast algorithm, precise remaking, FIR filters, discrete time transformation and continuous time transformation.

Bi-orthogonal

Symmetry, Arbitrary regularity, compactly supported bi-orthogonal, arbitrary number of vanishing moments, accurate reproduction, FIR filters, bi-orthogonal analysis, continuous and discrete time transformation.

Reverse Bi-orthogonal

An arbitrary number of vanishing moments, symmetry, Arbitrary regularity, compactly supported bi-orthogonal, exact reconstruction, the existence of the scaling function, bi-orthogonal analysis, FIR filters, fast algorithm, continuous and discrete transform.

2.2.2.13 Maximum Overlap Wavelet Packet Transform (MOWPT)

According to Mallet, the co-efficient of discrete wavelet packet transform (DWPT) at level 'j' is calculated by convolving the sampled input with infinite impulse response of filter 'g' and 'h' are explained in Eqns. (2.17) and (2.18).

$$S_j^{2z}(K) = \sum_{n=-\infty}^{+\infty} g(n)\, s_{j-1}^{z}(2k-n) \qquad (2.17)$$

$$S_j^{2z+1}(K) = \sum_{n=-\infty}^{+\infty} h(n)\, s_{j-1}^{z}(2k-n) \quad (2.18)$$

Where S_0^0 is the input signal; where z = 2m is the number of nodes and m ϵ N at j level, m $\leq 2^{j-1}-1$; S_j^0(k) is the node zero segments used for the representation of decomposed packet coefficients at low recurrence band at j scale shown in Eqns. (2.19) and (2.20), whereas at another node, i.e., for z not equal to zero, S_j^z(k) represent another decomposition packet co-efficient at highest frequency band at scale 'j'. where 'g' is the scaling filter and 'h' is the wavelet filter which presents the accompanying qualities.

$$\sum_{n=-\infty}^{+\infty} g(n) = \sqrt{2}\,,\ \sum_{n=-\infty}^{+\infty} g^2(n) = 1\,,\ \sum_{n=-\infty}^{+\infty} g(n)\, h(n) = 0 \quad (2.19)$$

$$\sum_{n=-\infty}^{+\infty} h(n) = 0\,,\ \sum_{n=-\infty}^{+\infty} h^2(n) = 1\,,\ \sum_{n=-\infty}^{+\infty} g(n)\, h(n) = 0 \quad (2.20)$$

Using Eqns. (2.17) and (2.18), the coefficients of DWPT are concluded in samplings by utilizing the approach, i.e., a factor of two down-sample. The MOWPT divides the original signal in coefficients into indefinite levels that represent uniformity in frequency band output. For reconstruction of the signal, reverse convolution has been performed on the decomposed coefficients to the low pass and high pass filter. Eqns. (2.21-2.24) give the MOWPT divide and reconstruct the co-efficient at any level j.

$$S_j^{2z}(K) = \frac{1}{\sqrt{2}} \sum_{n=-\infty}^{+\infty} g(n)\, s_{j-1}^{z}(k-n) \quad (2.21)$$

$$S_j^{2z+1}(K) = \frac{1}{\sqrt{2}} \sum_{n=-\infty}^{+\infty} h(n)\, s_{j-1}^{z}(k-n) \quad (2.22)$$

$$a_{j-1}^{2z}(K) = \frac{1}{\sqrt{2}} \sum_{n=-\infty}^{+\infty} g(n)\, s_j^{2z}(n-k) \quad (2.23)$$

$$a_{j-1}^{2z+1}(K) = \frac{1}{\sqrt{2}} \sum_{n=-\infty}^{+\infty} h(n)\, s_j^{2z+1}(n-k) \quad (2.24)$$

The MOWPT algorithm has the upper hand over discrete wavelet packet transform (DWPT). It can additionally deteriorate the high-frequency signal and provide a higher response [D.K. Alves, 2017]. The process of decomposition of the ECG signal and reconstruction of the signal up to level 2 is shown in Figure 2.17. In this research work, MOWPT is also used to build rescaling of the filters, defining MOWPT is needed to conserve the energy i.e., $\widetilde{g_l} = \widetilde{g_l}/\sqrt{2}$ and $\widetilde{h_l} = \widetilde{h_l}/\sqrt{2}$ so that $\sum_{l=0}^{L-1} \widetilde{g_l}^2 =$

1/2 and the filters are the (QMFs) quadrature mirror filters. The wavelet filters must satisfy the given properties as given in Eqns. (2.25-2.26) [D.B. Percival and A.T. Walden, 2000].

$$\sum_{l=0}^{L-1} \widetilde{h_l} = 0 \qquad (2.25)$$

$$\sum_{l=0}^{L-1} \widetilde{h_l} = ½ = \sum_{l=0}^{L-1} \tilde{h}\, \widetilde{h_{l+2r}} = ½ \qquad (2.26)$$

For all the integers having a value non-zero, where (L) indicates the length of the wavelet filter. The scaling factor $\{\tilde{g}_l\}$ is needed to satisfy Eqn. (2.27) and $\sum_{l=0}^{L-1} \tilde{g}_l = 1$. Now let us consider a time series i.e $c_{0,n}^{(M)} = x_n$ and $d_{j,n}^{(M)}$ is the wavelet co-efficient generated by the MOWPT algorithm and the scaling coefficient $c_{j,n}^{(M)}$ from $c_{j-1,n}^{(M)}$ where M indicates MOWPT. This is a co-efficient having a non-zero value divided by $\sqrt{2}$, the convolution can be written by Eqn. (2.27).

$$d_{j,n}^{(M)} = \sum_{l=0}^{L-1} \widetilde{h_l}\, c_{j-1,(n-2^{j-1}l)}^{(M)} \bmod N \text{ and}$$
$$c_{j,n}^{(M)} = \sum_{l=0}^{L-1} \tilde{g}_l\, c_{j-1,(n-2^{j-1}l)}^{(M)} \bmod N \qquad (2.27)$$

Where 'n' lies between (0 to N-1), where N indicates the time-series duration to be calculated. The filter operation of the original time series $\{x_n\}$ can be calculated as circular given in Eqn. (2.28), after using the filter $\widetilde{h_{j,l}} = h_{j,l}/2^{j/2}$ and $\widetilde{g_{j,l}} = h_{j,l}/2^{j/2}$.

$$d_{j,n}^{(M)} = \sum_{l=0}^{L_j-1} \widetilde{h_{j,l} x_{n-l}} \bmod N \text{ and } c_{j,n}^{(M)} = \sum_{l=0}^{L-1} \widetilde{g_{j,l} x_{n-l}} \bmod N \qquad (2.28)$$

The original signal can be recalculated by using Eqn. (2.29) from $d_j^{(M)}$ and $c_j^{(M)}$ after usage of the inverse MOWPT algorithm.

$$c_{j-1,n}^{(M)} = \sum_{l=0}^{L-1} \widetilde{h_l}\, d_{j,(n+2^{j-1}\,l)}^{(M)} \bmod N + \sum_{l=0}^{L-1} \widetilde{g_l}\, c_{j,(n+2^{j-1}\,l)}^{(M)} \; mod\; N \qquad (2.29)$$

Where n= 0, 1 ……. N-1. The point to be noted is that the resolution j, the mean of the wavelet coefficients for the maximal overlap wavelet packet transform (MOWPT) $d_{j,n}^{(M)}$ having the value must be zero as shown in Eqn. (2.30).

$$E\ \{d_{j,n}^{(M)}\ \} = \sum_{l \in Z} \widetilde{h_{j,l}}\, E\ \{x_{n-l}\} \bmod N = 0 = \mu_x \sum \tilde{h}_{j,l} = 0 \qquad (2.30)$$

Where μ_x is the mean of a signal.

2.2.2.13.1 Algorithm for MOWPT

- Decompose the original ECG signal using MOWPT at various levels via low and high pass filters. The co-efficient of discrete wavelet packet transform (DWPT) at level 'j' is calculated by convolving the sampled input with IIR (impulse response filter) and 'g' & 'h' as given in Eqns. (2.17) and (2.18).
- The decomposed packet coefficients represent at lowest frequency band at 'j' scale as in Eqns. (2.17) and (2.18), Where S_0^0 is the original input signal; where z = 2m is the quantity of nodes and m ϵ N at j scale, m $\leq 2^{j-1} - 1$; S_j^0(k) is the node zero segments used for the representation of decomposed packet co-efficient at low recurrence band at j scale shown in Eqns. (2.19) and (2.20), Whereas at another node, i.e., for z not equal to zero, S_j^z(k) represents another decomposition packet co-efficient at the highest frequency band at scale j.
- Perform reconstruction or synthesis; reverse convolution has been performed on the decomposed coefficients to the low pass and high pass filter to reconstruct the input signal.

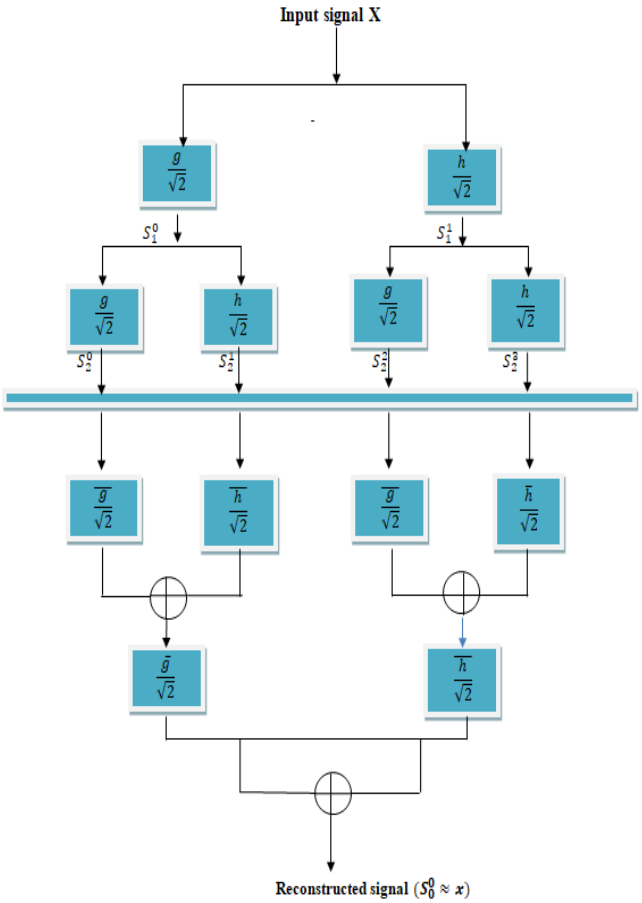

Figure 2.17 Process of decomposition and reconstruction using MOWPT (decomposition level is 2) [Reproduced from D.K. Alves, 2017]

2.3 Encryption and Authentication

2.3.1 Data Encryption Standard (DES)

It is employed to improve the flaws in DES without requiring the usage of another encryption scheme. The 56-bit key used by DES is insufficient for encrypting sensitive data. This encryption scheme is described in detail in Figure 2.18. The diagram illustrates that the initial permutation (IP) is given a 64-bit plaintext to regroup the bandwidth required to generate the permuted input. Following that, there is a stage with 16 rounds of the same function, including permutation and substitution functions. The sixteenth round's final product is made up of 64 bits, which are used to perform the functions of the input plaintext and the security key. The outputs of the left and right halves are swapped to generate pre-output, which then is given by an inverse permutation function of the initial permutation function used to create the 64-bit ciphertext [O. Rao, 2015].

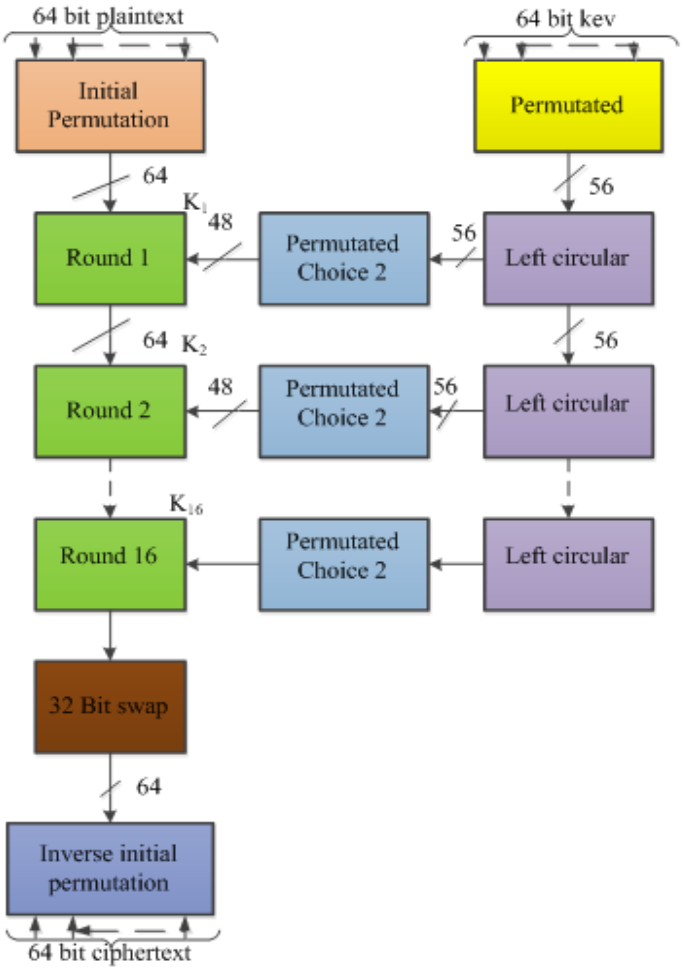

Figure 2.18 Description of Data Encryption Standard (DES) algorithm

[Reproduced from O. S.Rao, 2015]

2.3.2 Single Round Description

Figure 2.19 comprehensively describes the structural properties of the data encryption standard (DES) in a single round. The two halves of the 64 bits are considered the two separate 32-bit, labelled as the left and right. The complete processing of the round can be summed up using Eqn. (2.31) [O. S. Rao, (2015)]:

$$L_i = R_{i-1}$$
$$R_i = L_{i-1} \{F(R_{i-1}, K_i\} \quad (2.31)$$

The source 'R' is 32 bits long, while the key 'Ki' is 48 bits long. In this work, the significance of 'R' is increased to 48 bits to describe a possible combination with an expansion that yields an identical replica of 16 R bits. The output, which is 48 bits long, is then XORed with the key Ki. The 48-bit result is then fed into a replacement function, which produces a permuted 32-bit output. The substitution function is made up of S-boxes, each of which takes 6 bits as input and produces 4 bits as output.

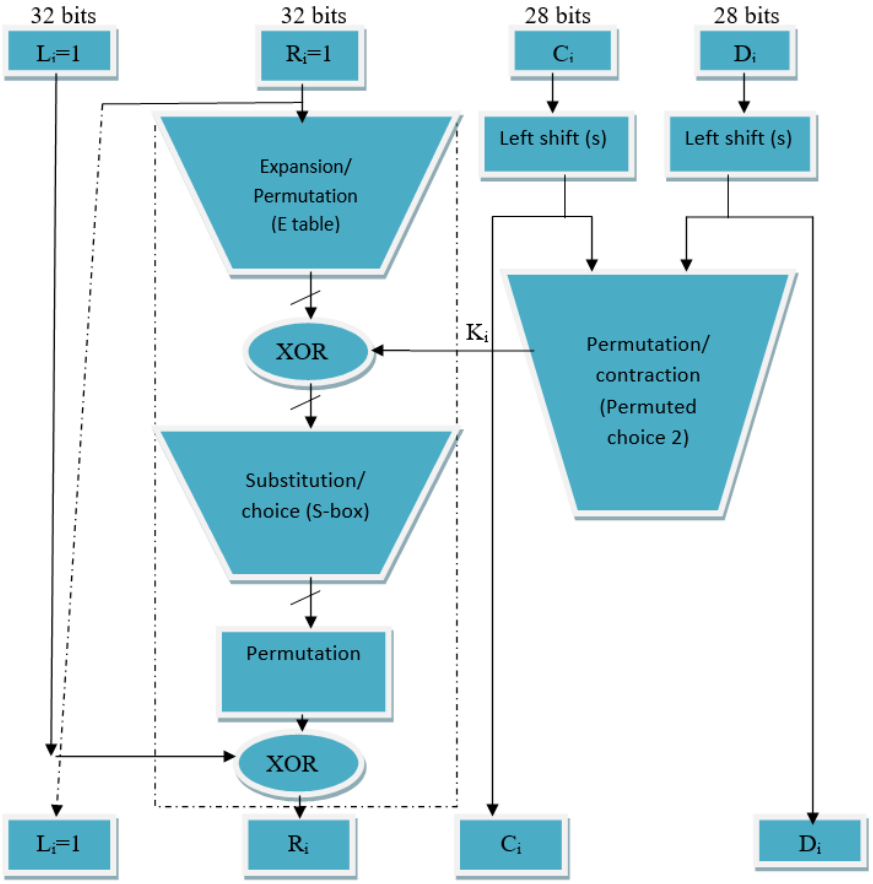

Figure 2.19 Depicts the internal workings of a single round of Data Encryption Standard [Reproduced from O. S.Rao, 2015]

2.3.3 Decryption with DES

The invertible encrypted message is decryption. The decryption process is the same as the encryption algorithm but with the inverted key added.

2.4 Data Security for ECG

The person's sensitive data trying to hide in the electrocardiogram (ECG) signal and its cryptography are emerging biometric security mechanisms. The electrocardiogram (ECG) includes crucial patient cardiovascular status information. It is subject to spoof attacks and violates HIPAA standards if sent without encryption. As a result, the ECG segments must be appropriately encrypted to prevent imposters from recording and getting unauthorized access to the secured facilities. To protect confidential patient data, [S. Abuadbba and A. Ibaida, 2019] proposed a wavelet-based steganography system that involves cryptography and scrambling. [H. Li, D. Yuan et al., 2017] proposed an efficient scheme for a health information system to preserve patients' personal privacy. Personal data was encrypted in the scheme before being contained in a health information system server's dataset. [M. U. Shaikh et al., 2018] authors proposed the FHE method, and in this signal, the processing is combined utilizing the QRS complex. The test is conducted to show that the ECG signal is safeguarded using the FHE approach. This approach encrypts and decrypts the ECG signal such that only a medical professional can decipher the outcome. The FHE algorithm is used for two threshold points to secure the ECG signal. No one can interpret the signal due to the encrypted threshold points. [R.R. Devi et.al, 2018]. In the presented work, we employed a triple Data Encryption Standard (3-DES) algorithm—a mix of the triple DES and anonymization algorithms— introduced. It was created with security in mind for big data in healthcare. The 3-DES algorithm enhances security. The proposed safe big data storage is implemented using Cloud sim on the JAVA working platform. This demonstrated the benefits of the triple DES approach, including improved accuracy and security during encryption and decryption. [X. Zhai et al., 2020] authors demonstrated the advanced encryption standard (AES) algorithm and electrocardiogram (ECG) identification system are two security solutions that can be implemented in a linked health environment. On the Xilinx ZC702 prototyping board, effective System-on-Chip (SoC) implementations of the suggested algorithms have been carried out. The proposed solutions employ just 30% of the hardware

resources and use 107 MW of power to process an ECG sample in 10.71ms. [M.E. Hameed et.al, 2020]. The primary goal of this work was to create a simple model for securely and effectively processing ECG readings. Five notable datasets from the MIT-BIH arrhythmia repository were processed using various techniques, including de-noising, compression, filtering, and encryption, to verify the effectiveness of the suggested model. The Huffman lossless technique was used because compressed signals need less processing time than raw signals. The authors achieved a compression rate of 35.015% using an algorithm, and the PRD is 0.411. The advantage was that the corrupted ECG appeared to be expected, despite being encrypted. The insertion of the key for decryption increased the entire ECG data size by 0.9 per cent, which was a restriction of employing this method. To secure patient rights information on the ECG, [B.Q. Chen et al., 2020] used quantization-based digital watermark encryption technology. An authentication of ECG data is addressed in this to protect personal information privacy. It obfuscates physiological data (ECG) by concealing and encrypting private data. Both ECG steganography and encryption approaches have been researched for this purpose.

Because ECG signals are millivolt signals, they are extremely sensitive. As a result, among the most pressing issues in the health service is that retaining vital data in an electrocardiogram signal and transmitting an electrocardiogram signal to a doctor must be highly secure. This aims to develop a one-time padding key that encrypts and authenticates data for confidentiality and authenticity. In ECG data transmissions, symmetric key algorithms are preferred over asymmetric key algorithms. There are numerous encryption algorithms in the literature, including advanced encryption standard (AES), data encryption standard (DES), triple data encryption standard (3-DES), Blowfish, Rivest–Shamir–Adleman (RSA), and others.

The triple-DES, on the other hand, uses less CPU processing time and memory [V. Goyal and A. Zafar, 2020], [G. Singh and Supriya, 2013]. Furthermore, the triple-data encryption standard was designed for hardware implementations, whereas the advanced encryption standard (AES) is better suited to both hardware and software implementations. In the same way, triple-DES is compatible and flexible with IoT systems. The electrocardiogram module uses a protocol for IoT systems, typically limited and expressed in memory and processing speed. Compared to AES-based

techniques, the Triple-data encryption standard (3-DES) requires large memory and power and is not necessarily appropriate for lightweight solutions (like IoT systems). In the proposed approach, we chose Triple data encryption standard (3-DES) as Internet of Thing (IoT) encryption, but AES should be investigated further. This was obtained through a water cycle optimization strategy that creates a random 56-bit one-time padding key for the electrocardiogram signal using the triple data encryption standard (3-DES) technique. An encryption and authentication approach was used to verify the data's accuracy. On conventional ECG data, an experiment was conducted, and several outcomes were determined. This approach has enhanced the confidentiality and static analysis key generation tests in this research work. The flow of this proposed data encryption approach is shown in Figure 2.20. Combine the ciphertext and the initialization vector (IV) key using the XOR technique. The output of the XOR was then provided to the encryption system, which resulted in the production ciphertext, along with the secret key. The ciphertext was generated by repeating the same process for every remaining plaintext data. Finally, the ciphertext block functions as an authentication tag, ensuring the plaintext's integrity and authentication. The steps in the suggested process are as follows:

Generalized Steps for Encryption Process

Step 1 Secured data and secret keys are input.

Step 2 Data encryption and authentication tag are the outputs.

Step 3 To begin, read the secret data and split it into 64-bit pieces.

Step 4 Examine the special code

Step 5 Using the water cycle approach, generate the initialization vector key (IV).

Step 6 The 3-DES algorithm is given the secret data block, secret key, and initialization key forencryption reasons.

Step 7 The encrypted data then serves as a (IV) key for the following block.

Step 8 Repeat steps 3–4 until all of the confidential data has been encrypted.

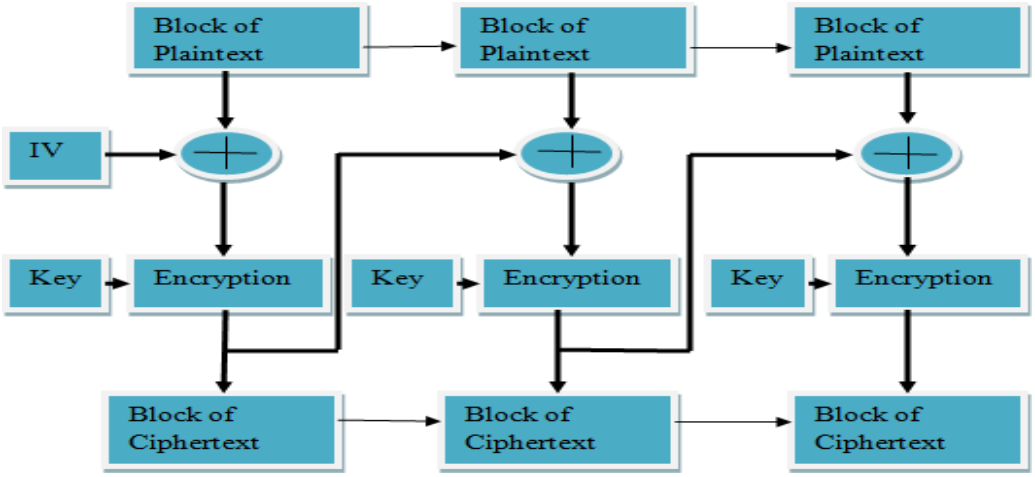

Figure 2.20 Process flow of the suggested data encryption method [Reproduced from V. Goyal and A. Zafar, 2020]

2.5 Water Cycle Optimization Process (WCO)

[A. Barzegar et al. (2019)] describe it as a meta-heuristic improved technique that processes natural water flow. Begin a rainfall or precipitation technique in this procedure; a random river or scheme factor population is generated in the range between the upper and bottom constraints. Figure 2.21 depicts the WCO flow diagram. [H. Eskandar et.al, 2012]. The minimum destination function value and the optimal flow with the stream acting as the sea are selected for the problem minimization. It is based on its desired value, the number of river classes to choose a river.

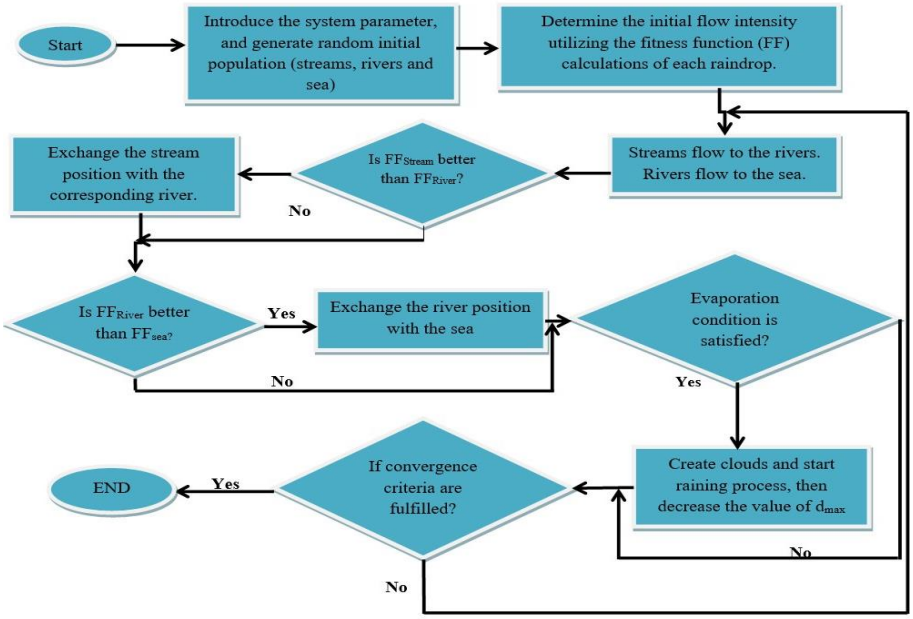

Figure 2.21 Flow scheme of Water cycle optimization [Reproduced from A. Barzegar et.al, 2019]

2.6 Internet of Things (IoT)

The Bluetooth low energy approach is used in the Internet of Things system that relies on the ECG module to transmit patient monitoring data in real-time to a smartphone running the Android operating system. Devices run the Electrocardiogram component, display electrocardiogram (ECG) data, and send electrocardiogram information to the server over the web. This server is used to access or store ECG data [S. Kumari, A. Dogra and R. Bhatt, 2018]. As seen in Figure 2.22, there are two parts to the data transmission protocol. The purpose of connecting Bluetooth in the first step is to create a low-power system that organizes ECG data. The TCP/IP protocol is used in the second stage to transfer ECG data from a smart device through the broadband system or a 4G system. Figure 2.23 depicts the internal layout of an IoT-based system; In this technique, the computer system acts as a conduit for the expert to retrieve the actual ECG data. The system also supports a network of clients (physician terminals) connected to the server via a smartphone and an ECG. Thing Speak, an open-source Internet of Things platform, uses cloud channels to identify heart problems. An Internet of Things (IoT) software called Thing Speak validates data warehousing and gets an ECG signal over the Internet.

Figure 2.22 Diagram of an Internet setup including sensors, an Electrocardiogram monitor, and a phone [Reproduced from S. Kumari, A. Dogra and R. Bhatt, 2018]

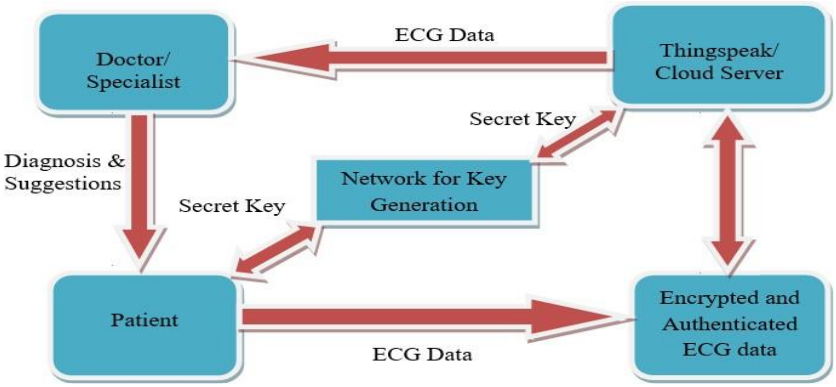

Figure 2.23 Drawing of an Internet - of - things network [Reproduced from S. Kumari, A. Dogra and R. Bhatt, 2018]

2.6.1 Components of an IoT System

The Internet of Things (IoT) does not have a universal definition; instead, different foundations and parties utilize different meanings. The Internet of Things (IoT) was defined as a general public worldwide data framework that allows interconnected objects to interact with one another and accomplish innovative capabilities using established and developing interconnected information communication technologies [N. Jumaa, 2017].

The Internet of Things (IoT) is an arrangement of associated gadgets. Figure 2.24 shows the parts of an IoT framework. Things in the Internet of Things (IoT) architecture have sensors to monitor their external elements and hardware for various purposes, including correspondence and programming for ethical considerations. Sensors monitor their surroundings in Internet of Things (IoT) frameworks, and data is sent to the cloud through Internet availability [N. Jumaa, 2017] [M. Sruthi and B.R. Kavitha, 2016].

People should be able to access high-quality medical care without time restrictions and from any location, at a low cost and with ease. The clinical consideration framework is going through a social shift from a regular to a modernized, patient-focused procedure. Healthcare experts play a vital role in the traditional approach; they must consult patients for essential evaluation and advice. This method has two significant things that could be improved. First and foremost, medical personnel must always remain on-site with the patient. Furthermore, the patient is assumed to be in a clinic and continuously connected to the instruments of point-of-care medical applications. These issues could be solved through the Internet of Things [A. Abdullah and A. Rashid et.al, 2015].

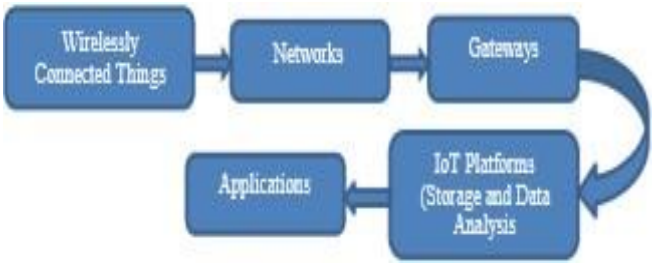

Figure 2.24 Components of IoT Systems [Reproduced from S. Kumari, A. Dogra and R. Bhatt, 2018]

An electrocardiogram (ECG) is a test used to measure the regular rhythm action of the heart condition. An electrocardiogram (ECG) signal represents heart activity to a

clinician by employing electrical impulses produced all through the heartbeat and recorded utilizing exterior electrodes. The medical importance of ECG in cardiology is well-known. To examine abnormal heart rhythms, use ECGs and figure out heart rates and the causes of chest pain. Electrodes are placed on a person's body, and heart action is monitored or graphed. A succession of electrical waves on the recorders represents each heartbeat. Peaks and valleys can be seen in the recorded waves, which are usually symbolized by the letters P, Q, R, S, T, and U, as shown in Figure 2.25 and ECG signal samples, as shown in Figure 2.26.

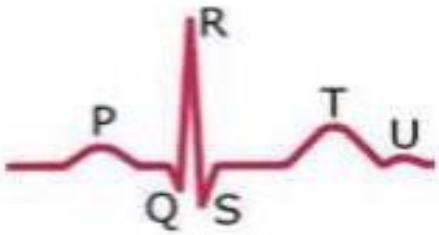

Figure 2.25 A healthy person's ECG signal [Reproduced from S. Kumari, A. Dogra and R. Bhatt, 2018]

This author presents and builds an IoT healthcare monitoring system using principal component analysis (PCA). The suggested IoT framework conveys the patients' ECG signals to an IoT cloud administration (ThingSpeak). To categorize heart disease, the Thing speak -MATLAB cloud data analysis method (PCA technique) compares the incoming signal to numerous ECG signals put away in the ThingSpeak channel data sets.

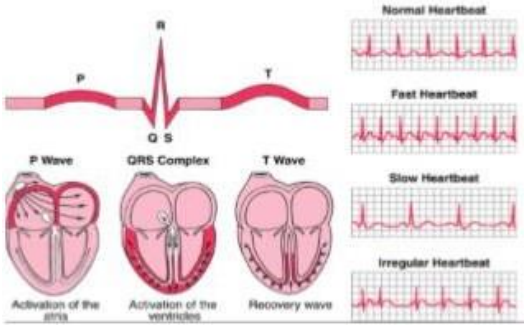

Figure 2.26 ECG signal samples [reproduced with permission from W.F. Ganong et al, 2005]

The MATLAB Context

MATLAB is an abbreviation for matrix laboratory. It has a multi-paradigm calculation environment and is a 4th generation computer program.

- MATH-Works in the United States is liable for the development of MATLAB.
- It enables the implementation and manipulation of algorithms, matrix visualization, data activelyplanning, the formation of a graphical user interface (GUI), and interconnects with programming languages.

MATLAB: Toolboxes are a family of application-oriented solutions. It also has the advantage of allowing the creation of reusable functions. The Customizable functions and programmers can be made effectively in MATLAB as code. Biomedical engineers use MATLAB to maintain the algorithm and propose medical equipment design and research. This product has a number of benefits over the conventional method, as given below:

There is no need to declare an array before using it for the first time. It enables rapid and simple programming in a high-level language. It requires very little attention. It allows quick improvisation and simple debugging.

MATLAB: M-files are easily transportable across an assortment of stages. It is possible to create high-quality visualization and graphics. For extension of the system, Toolboxes can be added.